A LETTERS JOURNAL EXPLORING THE FRONTIERS OF PHYSICS

January 2020

EPL, **129** (2020) 11002
doi: 10.1209/0295-5075/129/11002

www.epljournal.org

Testing texture two-zero neutrino mass matrices under current experimental scenario

MADAN SINGH

Department of Physics, M.N.S. Government College Bhiwani - Bhiwani, Haryana, 127021, India

received 11 November 2019; accepted in final form 21 January 2020
published online 12 February 2020

PACS 14.60.Pq – Neutrino mass and mixing
PACS 12.60.-i – Models beyond the standard model

Abstract – The latest data from the Planck Collaboration presented an improved sensitivity limit of the sum of neutrino masses (Σ), $\Sigma < 0.17$ eV at 95% confidence level (CL). On the other hand, the updated global fits of neutrino oscillation have shown a refined range of atmospheric mixing angle θ_{23} at the same CL. In the light of these observations, we have re-investigated the five viable cases ($B_{1,2,3,4}$ and C) of the texture two-zero Majorana mass matrix in the flavor basis. Using the present Planck's data, we have demonstrated that only cases B_2 and B_4 are now viable for normal mass ordering, while the remaining three cases do not meet the present experimental constraints at 2σ CL. The phenomenological predictions of the viable cases are also found to be in tune with the latest T2K, Super-Kamiokande and NOνA results, showing the preference for normal neutrino mass ordering ($m_1 < m_2 < m_3$), a maximal Dirac CP-violating phase ($\delta \simeq 270°$), and the upper octant of the neutrino mixing angle ($\theta_{23} > 45°$). In addition, the implication of Σ on the neutrinoless double beta decay is studied for viable cases.

Introduction. – Neutrino physics, at present, is going through a precision era as far as the physical parameters are concerned. In this regard, some notable progress has been seen in the recent past years, which triggers optimism in the lepton sector at significantly higher confidence level (CL). Thanks to three leading reactor neutrino experiments, Daya Bay, Double Chooz and RENO, the smallest mixing angle θ_{13}, also known as reactor angle, is measured at a precision level of 10% [1–5], which, in turn, not only opens up the possibilities to explore the leptonic CP violation, but is also helpful in pinning down the octant of atmospheric mixing angle θ_{23} [6] (which may be either $\theta_{23} > 45°$ or $\theta_{23} < 45°$ or even maximal, *i.e.*, $\theta_{23} = 45°$). The results obtained from T2K, Superkomiokande and NOνA experiments as well as the global fit analyses (see refs. [7–13]), in the recent past years, have shown some significant improvements regarding the Dirac CP-violating phase (δ), which is the measure of leptonic Dirac CP violation. The up-to-date data available from these experiments favors the maximal CP violation, $|\sin\delta| \sim 1$, with a significant preference for $\sin\delta < 0$. Referring to the updated global analysis [10], δ is found to be constrained within ∼15% (∼9%) uncertainty in the normal mass ordering (NO) (inverted mass ordering (IO)) around near maximal CP-violating values, $\delta \simeq 270°$, while $\delta \simeq 90°$ is now excluded at more than 4σ CL. On the other hand, the latest result obtained from NOνA experiment also provides strong indications regarding the octant of θ_{23}, excluding the maximal value of θ_{23}, *i.e.*, $\theta_{23} = 45°$, at 2.6σ CL [7]. The global fit analyses of neutrino oscillation reported in [8–10] indicate a slight preference for the upper octant ($\theta_{23} > 45°$) at $< 2\sigma$ CL, although both the octants are still favored at 3σ CL. In addition, for the first time, a considerable preference for NO over the IO has been reported at 3σ CL [9,10], with the help of coherent contribution from various data sets. The statistical data basically come from long-baseline accelerator experiments, and their interplay with short-baseline reactor experiments, where mass-ordering effects can be understood in terms of θ_{13}. The new data from T2K and NOνA experiments, possibly combined by the collaborations themselves [14], will further test the current trend favoring NO over IO in the present data sample.

Apart from the significant progress shown regarding the neutrino oscillation, new cosmological data from the Planck Collaboration [15] presented a refined limit,

$$\Sigma \equiv m_1 + m_2 + m_3 < 0.17\,\text{eV} \quad (\text{at } 95\%\ \text{CL}), \tag{1}$$

on the sum of neutrino masses (Σ). The above limit has been obtained in the framework of three degenerate neutrino masses and a ΛCDM model. The analysis has been done using the combination of the Planck temperature power spectrum with Planck polarization and the baryon acoustic oscillation data. On the other hand, KamLAND-Zen experiment found an improved limit for the neutrinoless double-beta ($0\nu\beta\beta$) decay [16], as $|M_{ee}| <$ (0.061–0.165) eV at 90% (or $< 2\sigma$) CL, where

$$|M_{ee}| = |m_1 c_{12}^2 c_{13}^2 e^{2i\rho} + m_2 s_{12}^2 c_{13}^2 e^{2i\sigma} + m_3 s_{13}^2|. \quad (2)$$

The effective mass, in eq. (2), is just the absolute value of the M_{ee} component of the neutrino mass matrix. The observation of the $0\nu\beta\beta$ decay, in the future, could determine the Majorana nature of neutrinos. For recent searches on the $0\nu\beta\beta$ decay see refs. [16–20]. The sensitivities of these searches correspond to mass scales in the so-called quasi-degenerate mass region. Further improvement will allow $|M_{ee}|$ to be probed below 50 meV, starting to constrain the inverted mass hierarchy region under the assumption that neutrinos are Majorana particles.

The above statistical data from different neutrino related experiments have been taken at considerably higher CL, and hence appear to be promising as far as exploring the flavor structure of the neutrino mass matrix is concerned. The construction of the mass matrix is necessary for model building, which, in turn, may unravel the underlying dynamics of neutrino masses, mixing and CP violation. In this context, the texture zero approach has been widely followed in the literature. In particular, texture two zeros have been relatively more successful in both flavor as well as in non-flavor basis [21–27]. Apart from higher predicting power among the textures zeros, two-zero mass matrices, in the flavor basis, can easily result from underlying flavor symmetries [28,29] and, in addition, can be realized within the framework of the see-saw mechanism [29,30]. Moreover, they can, also, be obtained in the context of GUTs based on SO(10) [31]. Thus, the study of texture two zeros is highly motivated on theoretical fronts.

The present neutrino oscillation data allows only seven out of the total fifteen cases of texture two-zero mass matrices at 3σ CL, as also shown earlier in refs. [23–27]. Out of these seven cases, A_1 and A_2 predict $|M_{ee}| = 0$, while $B_{1,2,3,4}$ and C predict non-zero $|M_{ee}|$, for the neutrinoless double-beta decay. Therefore, the present analysis is restricted to the following cases:

$$B_1\colon \begin{pmatrix} \times & \times & 0 \\ \times & 0 & \times \\ 0 & \times & \times \end{pmatrix}, \quad B_2\colon \begin{pmatrix} \times & 0 & \times \\ 0 & \times & \times \\ \times & \times & 0 \end{pmatrix},$$

$$B_3\colon \begin{pmatrix} \times & 0 & \times \\ 0 & 0 & \times \\ \times & \times & \times \end{pmatrix}, \quad B_4\colon \begin{pmatrix} \times & \times & 0 \\ \times & \times & \times \\ 0 & \times & 0 \end{pmatrix}; \quad (3)$$

$$C\colon \begin{pmatrix} \times & \times & \times \\ \times & 0 & \times \\ \times & \times & 0 \end{pmatrix}, \quad (4)$$

in order to study the implication for neutrinoless double-beta decay. The nomenclature has been used from ref. [23]. Using the experimental constraints, it was found, in earlier analyses [23,24], that all the five cases predict the quasi-degenerate neutrino mass spectrum. Earlier in ref. [32], Grimus showed that in the limit of quasi-degenerate neutrino mas spectrum, cases B_3 and B_4 lead to maximum atmospheric mixing angle. However, this prediction holds true irrespective of the experimental range of the solar and reactor mixing angle.

The purpose of the present work is to upgrade the analysis of Meloni *et al.* [25] in the light of the latest neutrino oscillation data, Planck Collaboration data as well as KamLAND-Zen data. Earlier, Meloni *et al.* carried out a detailed analysis of five cases ($B_{1,2,3,4}, C$) pertaining to two-zero Majorana mass matrix at 1σ CL. However, the improved limit of Planck's satellite data as well as the updated global fit analysis of neutrino oscillation warrant the re-examination of texture two-zero cases. Among the five cases, we find that only two (B_2 and B_4), for NO, are now compatible with the new data at 2σ CL, while the remaining cases are now ruled out at the same level. To this end, we have explicitly shown the incompatibility of the cases through the correlation between Σ and θ_{23}. In comparison with the analysis of Meloni *et al.* [25], our predictions remain valid at relatively higher CL. In addition, the phenomenological predictions for the viable cases are found to be in good agreement with the results obtained from the T2K, Super-Kamiokande, NOνA as well as KamLAND-Zen experiments. Earlier in ref. [22], Verma carried out the analysis for Fritzsch-like texture four-zero lepton mass matrices, in the light of these experimental observations.

The rest of the analysis is organized as follows: in the following section, we discuss the methodology used to reconstruct the neutrino mass matrix and texture two zero conditions. In the third section, we present the numerical analysis using some analytical relations and correlation plots. In the final section, we summarize and conclude our work.

General formalism. – The effective Majorana neutrino mass matrix (M_ν) contains nine parameters comprising three neutrino masses (m_1, m_2, m_3), three mixing angles ($\theta_{12}, \theta_{23}, \theta_{13}$) and three CP-violating phases (δ, ρ, σ), which can, in general, be expressed as

$$M_\nu = UP \begin{pmatrix} m_1 & 0 & 0 \\ 0 & m_2 & 0 \\ 0 & 0 & m_3 \end{pmatrix} P^T U^T, \quad (5)$$

where U denotes a 3×3 unitary matrix consisting of three flavor mixing angles ($\theta_{12}, \theta_{23}, \theta_{13}$), and one Dirac CP-violating phase (δ). $P = \mathrm{diag}(e^{i\rho}, e^{i\sigma}, 1)$, is a diagonal phase matrix containing two Majorana CP-violating phases (ρ, σ). The neutrino mass matrix M_ν can be re-written as

$$M_\nu = U \begin{pmatrix} \lambda_1 & 0 & 0 \\ 0 & \lambda_2 & 0 \\ 0 & 0 & \lambda_3 \end{pmatrix} U^T, \quad (6)$$

where $\lambda_1 = m_1 e^{2i\rho}, \lambda_2 = m_2 e^{2i\sigma}, \lambda_3 = m_3$. For performing the present analysis, we consider the following parameterization of U, used by Xing in [23]:

$$U = \begin{pmatrix} c_{12}c_{13} & s_{12}c_{13} & s_{13} \\ -c_{12}s_{23}s_{13} - s_{12}c_{23}e^{-i\delta} & -s_{12}s_{23}s_{13} + c_{12}c_{23}e^{-i\delta} & s_{23}c_{13} \\ -c_{12}c_{23}s_{13} + s_{12}s_{23}e^{-i\delta} & -s_{12}c_{23}s_{13} - c_{12}s_{23}e^{-i\delta} & c_{23}c_{13} \end{pmatrix}, \quad (7)$$

where, $c_{ij} \equiv \cos\theta_{\mathrm{ij}}$, $s_{ij} \equiv \sin\theta_{ij}$.

Using eq. (6), any element M_{ab} in the neutrino mass matrix can be expressed as

$$M_{ab} = \sum_{i=1,2,3} U_{ai} U_{bi} \lambda_i. \quad (8)$$

For two-zero texture, we consider only two elements of M_ν to be zero, simultaneously. Hence we obtain two constraints from eq. (8). Using them, we can derive the neutrino mass ratios (α, β) in terms of mixing matrix elements [24]. The three neutrino masses (m_1, m_2, m_3) can then be determined in terms of α, β as

$$m_3 = \sqrt{\frac{\delta m^2}{\beta^2 - \alpha^2}}, \qquad m_2 = m_3\beta, \qquad m_1 = m_3\alpha, \quad (9)$$

where δm^2 denotes the solar neutrino mass squared difference.
Using eq. (9), we can express Σ in terms of neutrino mass ratios as

$$\Sigma = \sqrt{\frac{\delta m^2}{\beta^2 - \alpha^2}}(\alpha + \beta + 1). \quad (10)$$

As we know, θ_{23} is known to be the most ambiguous among the three neutrino mixing angles, considering the long-standing octant problem. Therefore, in the context of the present analysis, it is useful to deduce Σ in terms of atmospheric mixing angle θ_{23} with the help of eq. (10).

The quasi-degenerate masses of neutrinos implies either $m_1 \lesssim m_2 \sim m_3$, for NO, or $m_3 \sim m_1 \lesssim m_2$, for IO. Following this assumption, we can express $|M_{ee}|$ explicitly in terms of Σ as

$$|M_{ee}| \simeq \frac{\Sigma}{3} |c_{12}^2 c_{13}^2 e^{2i\rho} + s_{12}^2 c_{13}^2 e^{2i\sigma} + s_{13}^2|. \quad (11)$$

The general relations in eqs. (10) and (11) will help to understand the phenomenological results of the present analysis.

Table 1: The updated global fits of neutrino oscillation data presented at 1σ, 2σ and 3σ CL. NO (IO) refers to normal (inverted) neutrino mass ordering [8].

Parameter	Best fit	1σ	2σ	3σ
δm^2 (10^{-5}eV^2)	7.55	7.39–7.75	7.20–7.94	7.05–8.14
$\lvert\Delta m^2_{31}\rvert$ (10^{-3}eV^2) (NO)	2.50	2.47–2.53	2.44–2.57	2.41–2.60
$\lvert\Delta m^2_{31}\rvert$ (10^{-3}eV^2) (IO)	2.42	2.38–2.45	2.34–2.47	2.31–2.51
θ_{12}	34.5°	33.5°–35.7°	32.5°–36.8°	31.5°–38°
θ_{23} (NO)	47.7°	46°–48.9°	43.1°–49.8°	41.8°–50.7°
θ_{23} (IO)	47.9°	46.2°–48.9°	44.5°–48.9°	42.3°–50.7°
θ_{13} (NO)	8.45°	8.31°–8.61°	8.2°–8.8°	8.0°–8.9°
θ_{13} (IO)	8.53°	8.38°–8.67°	8.3°–8.8°	8.1°–9.0°
δ (NO)	218°	191°–256°	182°–315°	157°–349°
δ (IO)	281°	254°–304°	229°–328°	202°–349°

Numerical analysis. – The experimental data regarding the neutrino oscillation parameters at 1σ, 2σ and 3σ CL, respectively, is given in table 1.

For carrying out the analysis, we scan the input neutrino oscillation parameters $(\theta_{12}, \theta_{23}, \theta_{13})$ and the mass squared differences $(\delta m^2, \Delta m^2)$ by allowing their random variation within their 3σ CL ranges. The Dirac CP-violating phase δ is allowed to vary from 0° to 360°. Before discussing further, we, again, emphasize here that all the seven texture zero cases are still allowed at 3σ CL.

In the following discusion, we explicate the phenomenological results through the correlation of Σ and θ_{23} for the texture two-zero cases. For the sake of comparison, we also provide the result at relatively higher limit, $\Sigma < 0.23$ eV [33], as used by Meloni *et al.* in [25]. The correlation plots of Σ and θ_{23} for all the five viable cases, have been complied in figs. 1, 2, 5.

Further, we provide the approximate analytical relations of Σ, as a function of θ_{23} using eq. (10). With the help of these expressions, we attempt to show analytically why a particular case is ruled out. To understand the implication of Planck's limit on the $0\nu\beta\beta$ decay, we relate the $|M_{ee}|$ with Σ analytically for the viable cases. The details of the analysis are presented as follows.

For cases B_1 and B_3, the approximate neutrino masses (m_1, m_2, m_3) can be expressed in the leading order of s_{13} as [23]

$$m_1 \simeq m_2 \simeq m_3 \tan^2\theta_{23}, \quad (12)$$

$$m_3 \simeq \sqrt{\frac{\Delta m^2}{1 - \tan^4\theta_{23}}}, \quad (13)$$

where Δm^2 denotes the atmospheric mass squared difference. From eq. (12), one can conclude that for $\theta_{23} > 45°$ ($\theta_{23} < 45°$), IO (NO) is allowed. Using eq. (13), as θ_{23} approaches to 45°, the three neutrino masses, m_1, m_2 and m_3, tend to infinite value, respectively. Hence, the recent cosmological scale rules out $\theta_{23} = 45°$ as is also evident in figs. 1 and 2.

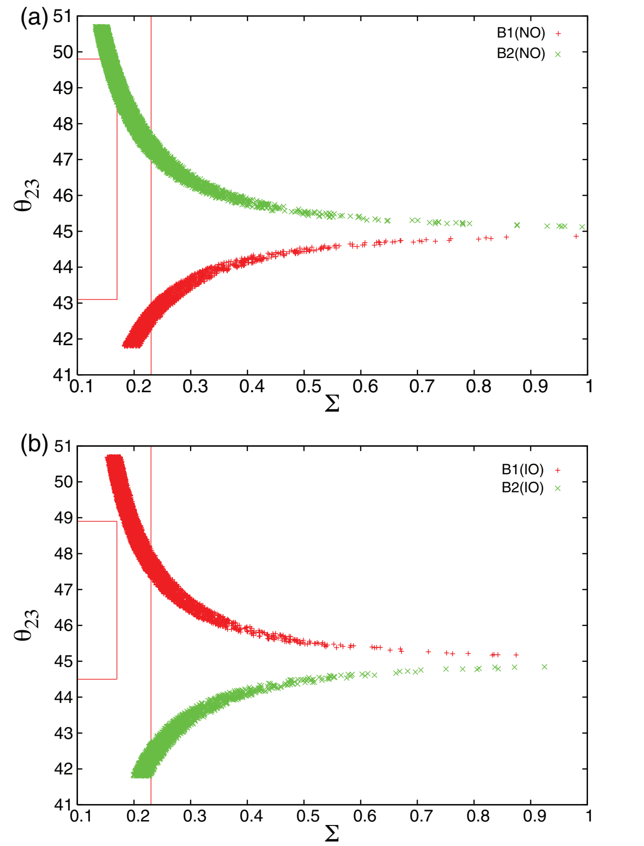

Fig. 1: Correlation plots between sum of neutrino masses, Σ (eV), and atmospheric mixing angle, θ_{23} (degree), for cases B_1 (red) and B_2 (green). The plots (a) and (b) correspond to NO and IO, respectively. The box shows the allowed parameter space at 2σ CL, while the solid line indicates the Planck's limit, $\Sigma = 0.23\,\text{eV}$.

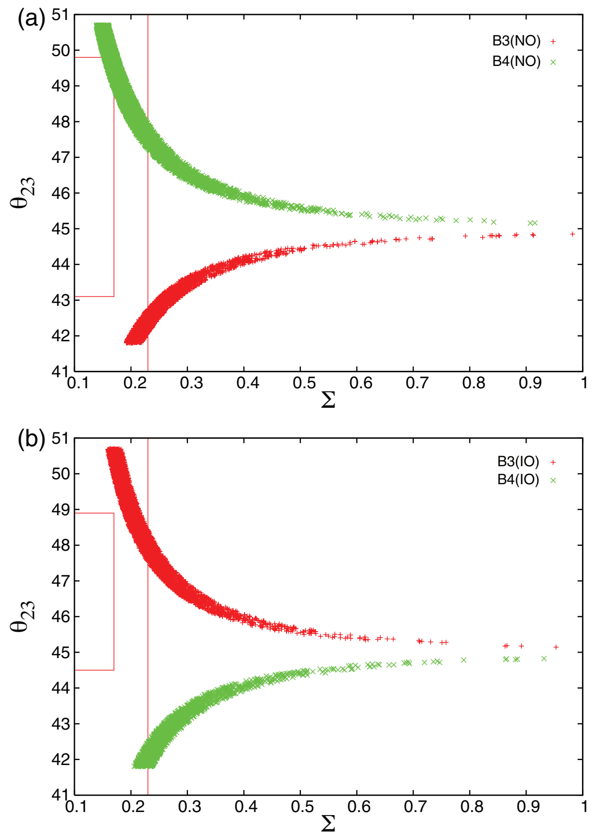

Fig. 2: Correlation plots between sum of neutrino masses, Σ (eV), and atmospheric mixing angle, θ_{23} (degree), for cases B_3 (red) and B_4 (green). The plots (a) and (b) correspond to NO and IO, respectively. The box shows the allowed parameter space at 2σ CL, while the solid line indicates the Planck's limit, $\Sigma = 0.23\,\text{eV}$.

Using eqs. (12) and (13), we can find Σ in terms of θ_{23} in the leading-order term

$$\Sigma \simeq \sqrt{\frac{\Delta m^2}{1-\tan^4\theta_{23}}}(2\tan^2\theta_{23}+1). \tag{14}$$

Using the 2σ range of neutrino oscillation data (table 1), we find, $\Sigma_{min} \simeq 0.24\,\text{eV}$, for NO. Hence, cases B_1 as well as B_3 are, now, ruled out for NO. The observation can be validated from figs. 1(a) and 2(a), showing the correlation between Σ and θ_{23}, for cases B_1 and B_3, respectively. On the other hand, for IO, $\Sigma_{min} \simeq 0.22\,\text{eV}$, which remains excluded in the scenario of the present limit on Σ. In figs. 1(b) and 2(b), we have shown the correlation between Σ and θ_{23} for cases B_1 and B_3, respectively, for IO. It is explicitly shown that the allowed parameter space is excluded by the present limit on Σ. On the contrary, the parameter space for cases B_1 and B_3, respectively, lies within the region of experimental bound, $\Sigma < 0.23\,\text{eV}$. Hence cases B_1 and B_3 are now ruled out for both NO and IO at 2σ level.

Similarly, for cases B_2 and B_4, we have presented the expressions for m_1, m_2 and m_3 in the leading order of s_{13} as [23]

$$m_1 \simeq m_2 \simeq m_3\cot^2\theta_{23}, \tag{15}$$

$$m_3 \simeq \sqrt{\frac{\Delta m^2}{1-\cot^4\theta_{23}}}. \tag{16}$$

Similar to cases B_1 and B_3, $\theta_{23} = 45°$ is ruled out for cases B_2 and B_4 as well, while $\theta_{23} > 45°$ ($\theta_{23} < 45°$) leads to NO (IO). Using eqs. (15) and (16), we can write

$$\Sigma \simeq \sqrt{\frac{\Delta m^2}{\tan^4\theta_{23}-1}}(2+\tan^2\theta_{23}). \tag{17}$$

Taking into account the 2σ range of neutrino oscillation parameter (table 1), we find, $\Sigma_{min} \simeq 0.154\,\text{eV}$ for NO, which lies in the range of Planck's limit. In fig. 1(a), we present the correlation between Σ and θ_{23} for case B_2 for NO. On comparing, we find that although both the cosmological limits allow the parameter space of θ_{23}, however for $\Sigma < 0.17\,\text{eV}$, the parameter space for the same is now reduced to an appreciable extent. More explicitly, $\theta_{23} < 45°$ is disallowed for NO.

Using 2σ CL of neutrino oscillation data, we get $\Sigma_{min} \simeq 0.24\,\text{eV}$ from eq. (17), for IO, which clearly lies outside the

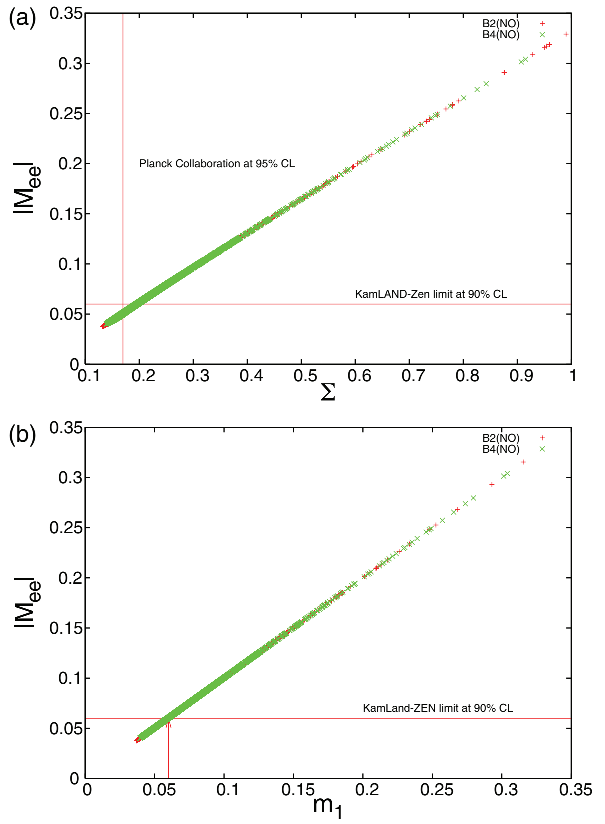

Fig. 3: (a) Correlation plots between sum of neutrino masses, Σ (eV), and effective mass term, $|M_{ee}|$ (eV), for cases B_2 (red) and B_4 (green) for NO. The vertical red line indicates the recent Planck Collaboration limit, while the horizontal line indicates the recent KamLAND-ZEN limit at 90% CL. (b) Correlation plots between lightest neutrino mass, m_1(eV), and effective mass term, $|M_{ee}|$ (eV), for cases B_2 (red) and B_4 (green) for NO. The solid bold line indicates the region for recent KamLAND-ZEN limit at 90% CL, and the vertical arrow points towards the upper bound on m_1.

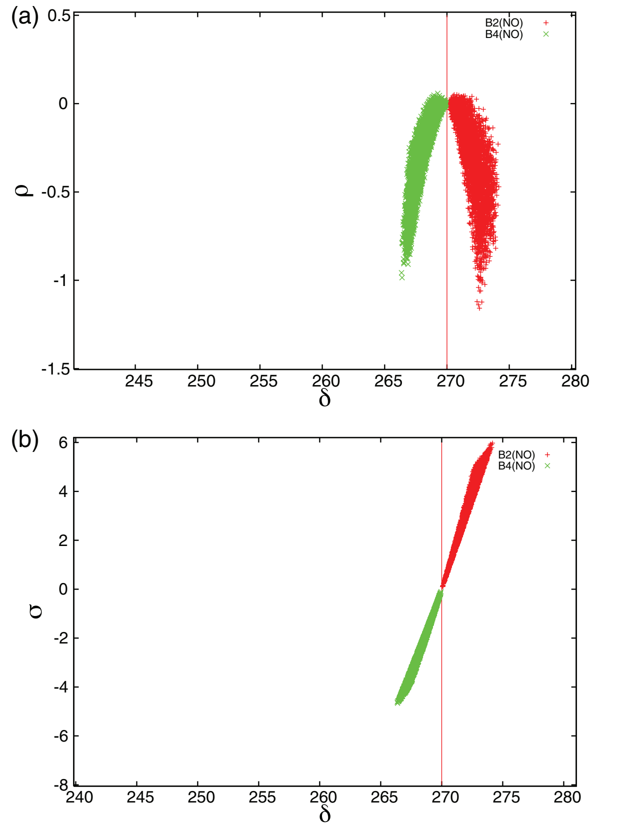

Fig. 4: Correlation plots between Majorana phases, ρ, σ (degree), and Dirac CP-violating phase, δ (degree), for cases B_2 (red) and B_4 (green) for NO, respectively.

present Planck's limit. Similar phenomenological results can be obtained for case B_4 for both NO and IO. The correlation plots have been compiled in figs. 1, 2, for the sake of completion. Earlier, Meloni *et al.* [25] also pointed out similar predictions for cases B_2 and B_4, respectively, at 1σ CL. In comparison with their results, our numerical result is compatible at relatively higher CL, and also the available parameter space of θ_{23} for NO is more constricted in our analysis.

Mathematically, one can relate the effective mass $|M_{ee}|$ in terms of Σ and θ_{23} using eq. (11):

$$|M_{ee}| \simeq \frac{\Sigma}{3} \cot^2 \theta_{23}. \tag{18}$$

The above relation has been obtained in the leading-order term of θ_{13}. Using the best fit of θ_{23}, $\theta_{23} = 47.7^\circ$, we find $|M_{ee}| < 0.0684\,\text{eV}$. This bound for $|M_{ee}|$ is found to be very close to the sensitivity limit obtained from KamLAND-Zen experiment (*i.e.*, $|M_{ee}| \leq 0.06\,\text{eV}$ [16]). The strong correlation between Σ and $|M_{ee}|$ also verifies this prediction on $|M_{ee}|$ (fig. 3(a)). Hence, our result for case B_2 resonates with the experimental bound of KamLAND-Zen experiment. In fig. 3(b), a strong linear correlation between effective mass $|M_{ee}|$ and lightest neutrino mass, m_1, have been shown indicating the quasi-degenerate spectrum for cases B_2 and B_4, respectively. It is clear that a significantly larger part of the parameter space above the sensitivity limit of KamLAND-Zen experiment is, now, ruled out. Figure 3(b) also puts the bound on the lightest neutrino mass, $m_1 \lesssim 0.06\,\text{eV}$, for cases B_2 and B_4, respectively.

In table 1, δ ranges from 157° to 349° for NO, and 202° to 349° for IO at 3σ CL. This new result automatically excludes the parameter space around $\delta \simeq 90^\circ$ and allows $\delta \simeq 270^\circ$ for cases B_2 and B_4. In figs. 4(a), (b), as δ is approaching to 270°, Majorana phases (ρ, σ) also approach to the vanishing value, otherwise $\rho \simeq 0^\circ, \sigma \simeq 0^\circ$ even at 3σ CL. In comparison with earlier analyses [23–27], our results for δ overlap with the recent global fits on δ [14], and also hold true at significant CL.

In the present scenario of analysis, the viable cases B_2 and B_4 seem to be very interesting from the experimental point of view since they simultaneously incorporate the updated T2K, Super-Kamiokande and NOνA results. The combined results favor the NO $(m_1 < m_2 < m_3)$, $\delta \simeq 270^\circ$ and $\theta_{23} > 45^\circ$ at higher CL. Earlier in ref. [26],

Table 2: Predictions regarding the current status of five viable cases along with the allowed parameter space of the octant of θ_{23}, Dirac CP-violating phase (δ), effective neutrino mass ($|M_{ee}|$), and sum of neutrino masses (Σ) at 2σ CL.

Cases	NO				IO			
	Octant	δ	$\lvert M_{ee}\rvert$	Σ	Octant	δ	$\lvert M_{ee}\rvert$	Σ
B_1	×	×	×	×	×	×	×	×
B_2	$\theta_{23} > 45°$	270.05°–273.2°	$\lvert M_{ee}\rvert > 0.0389$ eV	$\Sigma > 0.141$ eV	×	×	×	×
B_3	×	×	×	×	×	×	×	×
B_4	$\theta_{23} > 45°$	267.25°–270°	$\lvert M_{ee}\rvert > 0.0422$ eV	$\Sigma > 0.151$ eV	×	×	×	×
C	×	×	×	×	×	×	×	×

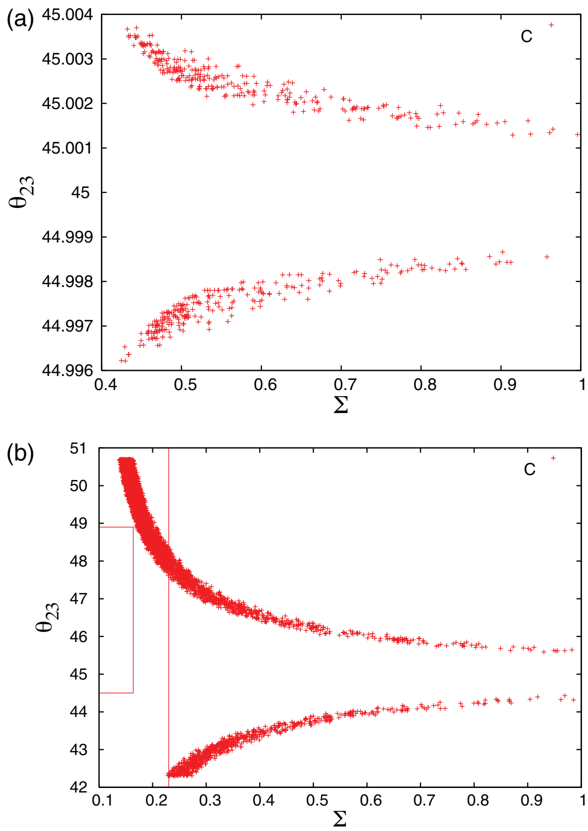

Fig. 5: Correlation plots between sum of neutrino masses, Σ (eV), and atmospheric mixing angle, θ_{23} (degree), for case C for (a) NO (b) IO. The box indicates the allowed parameter space at 2σ CL. The vertical line indicates the Planck's limit, $\Sigma = 0.23$ eV.

Zhou also discussed similar predictions for these cases along with cases A_1 and A_2, respectively, at 1σ CL.

The phenomenological implications of B_2 and B_4 are almost similar regarding the neutrino mass ordering, octant of θ_{23} and Dirac CP-violating phase (δ), therefore it seems to be difficult to differentiate them at low energies. To this end, we have to measure the CP-violating phase as precisely as possible, *e.g.*, an accuracy less than 1° is required if $\delta \simeq 270°$ is confirmed. Further, it may be possible that the phenomenological predictions for these cases come out to be different for the flavor models at high energy scale.

For case C, we can rewrite the expressions for Σ, as presented in [25]

$$\Sigma = \sqrt{\Delta m^2}\,\frac{[3 - s_{13}^2(2-\cos 2\delta)]}{2 s_{13}|\cos\delta|}, \qquad (19)$$

for NO if maximal θ_{23} is considered, while, for IO,

$$\Sigma \simeq \frac{\sqrt{\delta m^2}}{2}\left[\frac{2}{s_{12}^2} - \frac{2 s_{13} c_{12} t_{2(23)}}{s_{12}}\left(-1 + \frac{c_\delta}{s_{12}^2}\right) + s_{13}^2\left(\frac{(-2c_\delta c_{12}^2 + 1)}{s_{12}^2} + \frac{c_\delta^2(3c_{12}^2 - s_{12}^2)t_{2(23)}^2}{s_{12}^4}\right)\right], \qquad (20)$$

where $t_{2(23)} \equiv \tan 2\theta_{23}$, $c_\delta \equiv \cos\delta$. The analysis done by Meloni *et al.* [25] excludes the NO for case C at 1σ CL, which also remains consistent with our result (fig. 5(a)). Using the 2σ range of neutrino oscillation parameters, from eq. (20), we find, $\Sigma_{min} \simeq 0.174$ eV, which marginally lies outside the current Planck's limit, $\Sigma < 0.17$ eV. This indicates that case C is now ruled out for IO as well. This result is different from that of ref. [25], which allows IO for case C. To comprehend this result, we have presented the comparison, considering the Planck's limit, $\Sigma < 0.17$ eV and $\Sigma < 0.23$ eV, respectively (figs. 5(b)). The correlation between Σ and θ_{23} clearly excludes the allowed parameter space for $\Sigma < 0.17$ eV, owing to the present refinement in θ_{23} and Σ at 2σ CL.

It must be noted that, even at 3σ CL, the parameter spaces of all the five cases are found to be tightly constrained under the current experimental scenario, as is evident from figs. 1–5; however no specific conclusion can be made regarding the physical parameters. In table 2, we have encapsulated the current status of texture two zero cases as well as the predictions on Σ, $|M_{ee}|$, δ in light of latest experimental data at 2σ CL.

Summary and conclusions. – To summarize our discussion, we have presented the complete analysis of texture two-zero Majorana mass matrices in the light of the combined results of latest neutrino oscillation experiments, Planck Collaboration as well as KamLand-Zen experiments. For the analysis, we have considered only five out of the seven viable cases; among them, only two cases (B_2 and B_4) with NO are found to be consistent with the combined data, while the remaining three cases (B_1, B_3 and C) are now ruled out for both NO and IO at 2σ CL. More importantly, the phenomenological results of the viable cases remain in tune with current observations of T2K, Super-Kamiokande and NOνA experiments. In addition, for the viable cases, the predictions for the effective mass term $|M_{ee}|$ is also found to be consistent with the latest KamLAND Zen limit on the neutrinoless double-beta decay. In the future, the precise measurement of δ might serve as an important discriminator for the viable two-zero textures.

To conclude our discussion, we would like to say that these predictions are exciting as far as the present experimental scenario is concerned. The further progress and precision in the statistical data from long-baseline experiments, cosmological as well as KamLand-Zen experiments could help us to validate these predictions regarding the two-zero texture at a significantly higher confidence level. This, as a consequence, can give us new insight into the structure of lepton mass matrices, and possibly help us to shed some light on the origin of neutrino masses and dynamics of flavor mixing and leptonic CP violation.

* * *

The author would like to thank the Principal of M. N. S. Government College, Bhiwani, Haryana, India, for providing the necessary facilities to work.

Data availability: The data used to support the findings of this study is included within this article.

Conflicts of interest: The author declares that there are no conflicts of interest regarding the publication of this paper.

REFERENCES

[1] T2K Collaboration (Abe K. *et al.*), *Phys. Rev. Lett.*, **107** (2011) 041801 (arXiv:1106.2822 [hep-ex]).
[2] MINOS Collaboration (Adamson P. *et al.*), *Phys. Rev. Lett.*, **107** (2011) 181802 (arXiv:1108.0015 [hep-ex]).
[3] Double Chooz Collaboration (Abe Y. *et al.*), *Phys. Rev. Lett.*, **108** (2012) 131801 (arXiv:1112.6353 [hep-ex]).
[4] Daya Bay Collaboration (An F. P. *et al.*), *Phys. Rev. Lett.*, **108** (2012) 171803 (arXiv:1203.1669 [hep-ex]).
[5] RENO Collaboration (Ahn J. K. *et al.*), *Phys. Rev. Lett.*, **108** (2012) 191802; Kim Soo-Bong, arXiv:1208.0626 [hep-ex].
[6] Bellini G. *et al.*, *Phys. Rev. Lett.*, **107** (2011) 141302 (arXiv:1104.1816 [hep-ex]).
[7] NOvA Collaboration (Adamson P. *et al.*), *Phys. Rev. Lett.*, **118** (2017) 231801 (arXiv:1703.03328 [hep-ex]).
[8] de Salas P. F., Forero D. V., Ternes C. A., Tortola M., Valle J. W. F., *Phys. Lett. B*, **782** (2018) 633 (arXiv:1708.01186 [hep-ph]).
[9] Capozzi F., Lisi E., Marrone A. and Palazzo A., arXiv:1804.09678 [hep-ph].
[10] Esteban I., Gonzalez-Garcia M. C., Hernandez-Cabezudo A. *et al.*, *JHEP*, **01** (2019) 106 (arXiv:1811.05487 [hep-ph]).
[11] Radovic A., *Latest Neutrino Oscillation Results from NOvA*, seminar at Fermilab (12 January 2018), available at `https://www-nova.fnal.gov`. See also the subsequent NOvA talks, up to March 2018.
[12] T2K Collaboration (Abe K. *et al.*), *Phys. Rev. D*, **96** (2017) 092006 (arXiv:1707.01048 [hep-ex]).
[13] Super-Kamiokande Collaboration, χ^2 *maps derived from full 3σ oscillations analysis*, `http://www-sk.icrr.u-tokyo.ac.jp/sk/publications/result-e.html`.
[14] *T2K and NOvA collaborations to produce joint neutrino oscillation analysis by 2021*, full announcement (30 January 2018) available at `http://t2k-experiment.org/2018/01/t2k-nova-announce/`.
[15] Planck Collaboration (Ade P. A. R. *et al.*), *Astron. Astrophys.*, **594** (2016) A13 (arXiv:1502.01589 [astro-ph.CO]).
[16] KamLAND-Zen Collaboration, *Phys. Rev. Lett.*, **117** (2016) 082503 (arXiv:1605.02889).
[17] Exo-200 Collaboration (Albert J. B. *et al.*), *Nature*, **510** (2010) 229 (arXiv:1402.6956 [nucl-ex]).
[18] Dell'oro S., Marcocci S., Viel M. and Vissani F., *Adv. High Energy Phys.*, **2016** (2016) 2162659 (arXiv:1601.07512).
[19] Rodejohann W., *Int. J. Mod. Phys. E*, **20** (2011) 1833 (arXiv:1106.1334 [hep-ph]).
[20] Avignone F. T. III, Elliott S. R. and Engel J., *Rev. Mod. Phys.*, **80** (2008) 481 (arXiv:0708.1033 [nucl-ex]); Gomez-Cadenas J. J., Martin-Albo J., Mezzetto M., Monrabal F. and Sorel M., *Riv. Nuovo Cimento*, **35** (2012) 29 (arXiv:1109.5515 [hep-ex]).
[21] Gupta M. and Ahuja G., *Int. J. Mod. Phys. A*, **26** (2011) 2973 and references therein.
[22] Verma Rohit, *Adv. High Energy Phys.*, **2016** (2016) 2094323 (arXiv:1607.00958 [hep-ph]).
[23] Frampton Paul H., Glashow Sheldon L. and Marfatia Danny, *Phys. Lett. B*, **536** (2002) 79 (hep-ph/0201008); Zhi-zhong Xing, *Phys. Lett. B*, **530** (2002) 159 (hep-ph/0201151).
[24] Fritzsch H., Xing Z. Z. and Zhou S., *JHEP*, **09** (2011) 083 (arXiv:1108.4534v2 [hep-ph]).
[25] Meloni D., Meroni A. and Peinado E., *Phys. Rev. D*, **89** (2014) 053009 (arXiv:1401.3207 [hep-ph]).
[26] Zhou Shun, *Chin. Phys. C*, **40** (2016) 033102 (arXiv:1509.05300 [hep-ph]).
[27] Singh Madan, Ahuja Gulsheen, Gupta Manmohan, *Prog. Theor. Exp. Phys.*, **2016** (2016) 123B08 (arXiv:1603.08083 [hep-ph]).
[28] Frampton P. H., Oh M. C. and Yoshikawa T., *Phys. Rev. D*, **66** (2002) 033007.
[29] Grimus Walter and Lavoura Luis, *J. Phys. G*, **31** (2005) 693.
[30] Grimus W., Joshipura A. S., Lavoura L. and Tanimoto M., *Eur. Phys. J. C*, **36** (2004) 227.
[31] Goh H. C., Mohapatra R. N. and Ng Siew-Phang, *Phys. Rev. D*, **68** (2003) 115008.
[32] Grimus W. and Ludl P. O., *Phys. Lett. B*, **700** (2011) 356 (arXiv:1104.4340 [hep-ph]).
[33] Planck Collaboration (Ade P. A. R. *et al.*), arXiv:1303.5076 [astro-ph.CO].